

## Electrical characterization of organic light-emitting diodes using dipotassium phthalate as n -type dopant

Meng-Huan Ho, Ming-Ta Hsieh, Teng-Ming Chen, Jenn-Fang Chen, Shiao-Wen Hwang, and Chin H. Chen

Citation: *Applied Physics Letters* **93**, 083505 (2008); doi: 10.1063/1.2976139

View online: <http://dx.doi.org/10.1063/1.2976139>

View Table of Contents: <http://scitation.aip.org/content/aip/journal/apl/93/8?ver=pdfcov>

Published by the [AIP Publishing](#)

---

### Articles you may be interested in

[Electronic structures of Ba-on- Alq 3 interfaces and device characteristics of organic light-emitting diodes based on these interfaces](#)

*J. Appl. Phys.* **105**, 083705 (2009); 10.1063/1.3106604

[Very low voltage and stable p - i - n organic light-emitting diodes using a linear S,S-dioxide oligothiophene as emitting layer](#)

*Appl. Phys. Lett.* **94**, 063510 (2009); 10.1063/1.3072798

[Incorporation of cobaltocene as an n -dopant in organic molecular films](#)

*J. Appl. Phys.* **102**, 014906 (2007); 10.1063/1.2752145

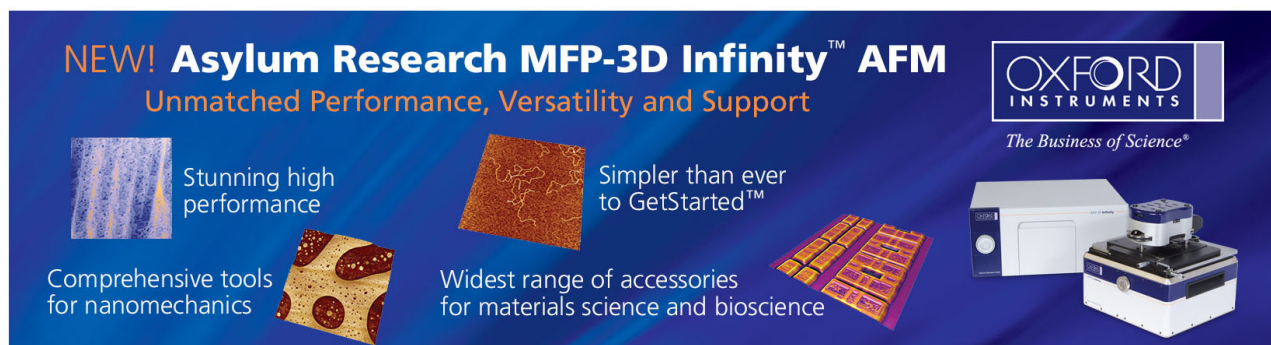
[Highly power efficient organic light-emitting diodes with a p -doping layer](#)

*Appl. Phys. Lett.* **89**, 253504 (2006); 10.1063/1.2405856

[Enhancement of hole injection using O 2 plasma-treated Ag anode for top-emitting organic light-emitting diodes](#)

*Appl. Phys. Lett.* **86**, 012104 (2005); 10.1063/1.1846149

---



**NEW! Asylum Research MFP-3D Infinity™ AFM**  
Unmatched Performance, Versatility and Support

**OXFORD INSTRUMENTS**  
*The Business of Science®*

Stunning high performance  
Simpler than ever to GetStarted™

Comprehensive tools for nanomechanics  
Widest range of accessories for materials science and bioscience

## Electrical characterization of organic light-emitting diodes using dipotassium phthalate as *n*-type dopant

Meng-Huan Ho,<sup>1,a)</sup> Ming-Ta Hsieh,<sup>2,a)</sup> Teng-Ming Chen,<sup>1</sup> Jenn-Fang Chen,<sup>2</sup> Shiao-Wen Hwang,<sup>3</sup> and Chin H. Chen<sup>3</sup>

<sup>1</sup>*Department of Applied Chemistry, National Chiao Tung University, Hsinchu, Taiwan 300, Republic of China*

<sup>2</sup>*Department of Electrophysics, National Chiao Tung University, Hsinchu, Taiwan 300, Republic of China*

<sup>3</sup>*Display Institute, Microelectronics and Information Systems Research Center, National Chiao Tung University, Hsinchu, Taiwan 300, Republic of China*

(Received 13 May 2008; accepted 31 July 2008; published online 26 August 2008)

An efficient *n*-doped electron transport layer composed of 4,7-diphenyl-1,10-phenanthroline (BPhen) and dipotassium phthalate (PAK2) has been developed. By temperature-dependent admittance spectroscopy, the incorporation of PAK2 into BPhen is found to raise the Fermi level from 1.7 eV to only around 0.5 eV below BPhen's lowest unoccupied molecular orbital, which further enhances the efficiency of electron injection from an Al cathode. When this *n*-doped layer is adopted in an organic light-emitting diode device, the green fluorescent 10-(2-benzothiazolyl)-1,1,7,7-tetramethyl-2,3,6,7-tetrahydro-1*H*,5*H*,11*H*-benzo[*l*]pyrano[6,7,8-*ij*]quinolizin-11-one doped device can achieve a current efficiency of 16 cd/A and a power efficiency of 10.9 lm/W at 1000 cd/m<sup>2</sup>. © 2008 American Institute of Physics. [DOI: 10.1063/1.2976139]

Since efficient organic light-emitting diodes (OLEDs) were discovered, developing OLEDs for display applications has attracted much attention.<sup>1,2</sup> Reducing the power consumption of OLEDs requires increasing the carrier injection from the electrode to the transporting layer. The commonly used strategy for electron injection into an electron transport layer (ETL) is to insert a thin lithium fluoride (LiF) interlayer between an Al cathode and a tris(8-hydroxyquinoline)aluminum (Alq<sub>3</sub>) layer.<sup>3</sup> The mechanism of electron injection into the LiF/Al composite cathode is a chemical reaction between Al and LiF.<sup>4</sup> Another class of electron injection materials is organometallic complexes with reactive metals such as lithium carboxylates<sup>5</sup> and 2-(hydroxy)quinoline lithium (Liq).<sup>6</sup> However, the effectiveness of these electron injection materials is very sensitive to the choice of metal, and only Al has been found to provide good device performance.

An alternative approach for an efficient carrier injection is to introduce a *p-i-n* structure into an OLED device, enabling the operating voltage to be considerably reduced in both fluorescent<sup>7</sup> and phosphorescent<sup>8</sup> systems. Highly conductive *n*-doped layers have been shown to enhance the injection of electrons from the contacts and to reduce the Ohmic losses in these layers. The most widely investigated *n*-type dopants for the ETL are alkali metals, such as cesium<sup>9</sup> and lithium.<sup>10</sup> However, they suffer from the necessity of a high doping ratio often of the order of 50% to achieve high conductivity, which often alters the host matrix properties. These methods require special equipments and care in handling reactive metals; they are thus not convenient for fabrication. In 2004, Canon Inc. reported that cesium carbonate (Cs<sub>2</sub>CO<sub>3</sub>),<sup>11</sup> either vacuum deposited as an individual layer over the organic electron transport material or codeposited with the organic electron transport material, facilitates elec-

tron injection from a wide range of metal electrodes. However, fabrication can be performed only at a high deposition temperature of Cs<sub>2</sub>CO<sub>3</sub> (around 500 °C under a vacuum). Therefore, finding a satisfactory *n*-type dopant with a low deposition temperature is important in developing OLEDs with low power consumption.

This letter develops an *n*-doped ETL that consists of dipotassium phthalate (PAK2) incorporated into 4,7-diphenyl-1,10-phenanthroline (BPhen) and the electrical characteristics by measuring current-voltage (*I*-*V*) and using temperature-dependent admittance spectroscopy (AS). PAK2 can grow at a stable rate at around 330 °C at a base vacuum of 10<sup>-7</sup> torr, significantly facilitating the fabrication process. A series of electron-only devices was also fabricated to study the electron injection and electrical characteristics. The electron-only device structure was indium tin oxide (ITO)/Alq<sub>3</sub> (60 nm)/*n*-doped ETL (30 nm)/Al (150 nm). In devices A, B, C, and D, the doping concentrations of PAK2 in BPhen as *n*-doped ETL were 0%, 5%, 10%, and 20%, respectively. To demonstrate that PAK2 is more effective than the conventional LiF/Al composite cathode, the following 10-(2-benzothiazolyl)-1,1,7,7-tetramethyl-2,3,6,7-tetrahydro-1*H*,5*H*,11*H*-benzo[*l*]pyrano-[6,7,8-*ij*]quinolizin-11-one (C-545T) green-doped OLED devices, whose structure was ITO/CF<sub>x</sub>/NPB (60 nm)/Alq<sub>3</sub>: 1% C545T (37.5 nm)/Alq<sub>3</sub> (37.5 nm)/electron injection layer (EIL)/Al (150 nm), was fabricated, while the EIL of devices I and II were LiF (1 nm) and BPhen: 5% PAK2 (5 nm), respectively.

Figure 1 plots the *I*-*V* characteristics of electron-only devices and reveals that the PAK2-doped devices B, C, and D all greatly outperform the undoped device A, indicating that doping PAK2 into BPhen promotes the injection of electron from the Al cathode. Device B with 5% PAK2 has better *I*-*V* characteristics than devices C and D, even at a small applied bias (inset in Fig. 1), probably due to the different extents of electron injection with various PAK2 doping concentrations. The electrical properties of this *n*-doped layer

<sup>a)</sup>Authors to whom correspondence should be addressed. Electronic addresses: kinneas.ac94g@nctu.edu.tw and mthsieh.ep94g@nctu.edu.tw.

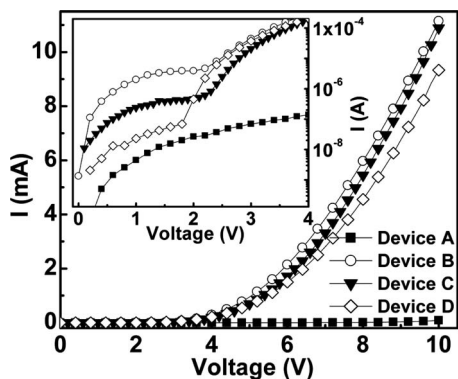


FIG. 1. Current-voltage ( $I$ - $V$ ) characteristics of electron-only devices in the linear scale. Inset: logarithmic scale under a small bias.

were investigated by temperature-dependent AS with an equivalent circuit model to elucidate this phenomenon. (Details of the methods and theories can be found elsewhere.)<sup>12-14</sup> Figure 2(a) depicts the 300 K capacitance-frequency ( $C$ - $F$ ) measured at 2 V and the conductance/frequency-frequency ( $G/F$ - $F$ ) spectra measured from 0 to 2 V on device B. The spectra show two capacitance drops and corresponding  $G/F$  peaks at the inflexion frequency. The  $G/F$ - $F$  spectra show a bias-independent peak at a high-frequency region, suggesting the presence of series resistances. They also show a bias-dependent peak at a low-frequency region, which is associated with the resistance of the BPhen layer. This argument is inferred from the observation that the  $C$ - $F$  spectra and  $G/F$ - $F$  spectra of devices C and D are similar to those of device B (not shown here). Device A shows only the bias-independent peak at the high-frequency region. In the  $C$ - $F$  spectra, the capacitance (4.7 nF) measured at 100 Hz corresponds to the thickness of the Alq<sub>3</sub> layer according to the parallel-capacitor model with a dielectric constant of 3.5.<sup>15</sup> As the frequency increases, the capacitance drops to a plateau whose value (3.2 nF) corresponds to a series combination of the Alq<sub>3</sub> and BPhen layers. Hence, the  $RC$  time constant of the BPhen can then be determined from the inflexion frequency. As the frequency further increases, the capacitance drops to zero, which is due to

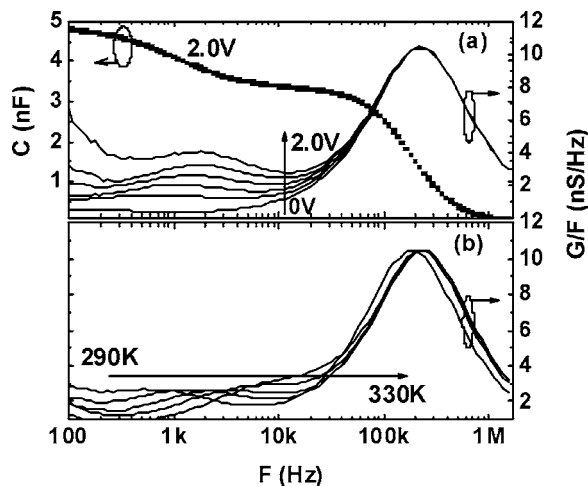


FIG. 2. (a) Capacitance-frequency ( $C$ - $F$ ) spectrum of device B at 2 V and conductance/frequency-frequency ( $G/F$ - $F$ ) spectra of device B from 0 to 2 V at room temperature; (b) temperature-dependent  $G/F$ - $F$  spectra of device B at 1.4 V.

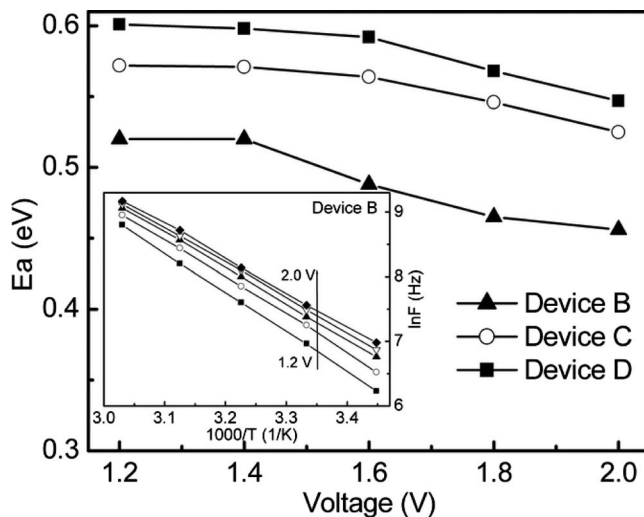


FIG. 3. Relationship between  $E_a$  and applied voltage of devices B, C, and D. Inset:  $\ln(F)$  vs  $1000/T$  at various biases for device B.

parasitic effects of lead/contact series resistances. The BPhen peak of the doped devices cannot be clearly detected at a bias of under 1 V because of a high energy barrier between Al and BPhen, limiting the AS measurements. The energy barrier becomes negligible as the bias is increased over 1 V, and therefore, the electrical properties of BPhen can be characterized. Moreover, the BPhen peak of the undoped device cannot be observed even at a high applied bias, suggesting that the energy barrier between the work function of Al (4.2 eV) and the lowest unoccupied molecular orbital (LUMO) of BPhen (2.9 eV) in device A is too high to be measured by AS. Figure 2(b) displays temperature-dependent  $G/F$ - $F$  spectra at 1.4 V for device B (the spectra at 1.2, 1.6, 1.8, and 2.0 V are similar to those at 1.4 V). The BPhen peak evidently depends significantly on temperature, and the series-resistance peaks are all independent of temperature. Furthermore, the frequency ( $F$ ) of the BPhen peak corresponds to the  $RC$  time constant of BPhen. Hence, the activation energy ( $E_a$ ) of the BPhen layer is given by a simple geometric equation,

$$F = F_0 \exp\left(\frac{-E_a}{KT}\right),$$

where  $F^0$  is the pre-exponential factor,  $E_a$  is the activation energy, which represents the energy separation between the edge of the Fermi level and the LUMO band,  $K$  is Boltzmann's constant, and  $T$  is the temperature. The inset in Fig. 3 plots  $\ln(F)$  versus  $1000/T$ , which yields the  $E_a$  value of the BPhen in device B at various biases. Figure 3 plots the relationship between  $E_a$  and the applied voltage of PAK2-doped devices. The calculated  $E_a$  values of the PAK2-doped devices are around 0.5–0.6 eV, which is much smaller than the  $E_a$  (half band-gap, 1.7 eV) of pure BPhen (the Fermi level of ideally pure organic semiconductors should be close to the middle of the gap).<sup>16</sup> Based on the AS results, the incorporation of PAK2 into BPhen increases the Fermi level of BPhen from deep to shallow, further reducing the interface energy barrier and increasing the efficiency of electron injection from the Al cathode. Moreover, device B has the smallest  $E_a$  value, according to AS, whose result agrees completely with the  $I$ - $V$  measurement. That increasing PAK2

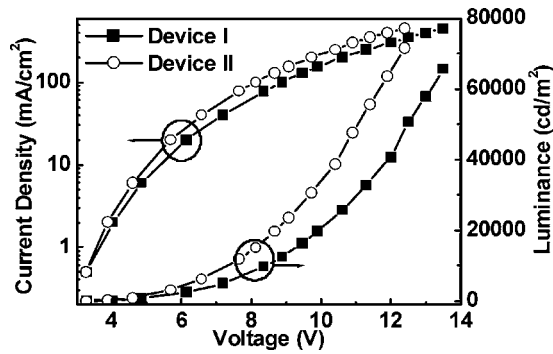


FIG. 4. Luminance-current density-voltage ( $L$ - $J$ - $V$ ) curves of devices I and II.

incorporation from 5% to 20% does not further improve the performance of electron injection is attributable to fallows from the effect of carrier quenching and defect generations.

Figure 4 plots the luminance-current density-voltage ( $L$ - $J$ - $V$ ) curves of devices I and II. Device II with  $n$ -doped ETL can achieve a higher current density and luminance at a lower voltage than device I with a conventional LiF/Al composite cathode. Device II achieved a power efficiency of 10.9 lm/W at 1000 cd/m<sup>2</sup> (16 cd/A at 4.6 V), which is 40% higher than that of conventional device I at 1000 cd/m<sup>2</sup> (7.8 lm/W and 12.7 cd/A at 5.0 V). These results clearly demonstrate that the  $n$ -doping effect of PAK2 in BPhen further enhanced the electron injection. The dominant carrier in most Alq<sub>3</sub>-based OLEDs is the injected hole.<sup>17</sup> The improvement of the electron injection from the cathode not only reduces the drive voltage but also balances the carrier recombination in the device, which we believe is the main reason for the enhanced efficiency of the device. The inset in Fig. 5

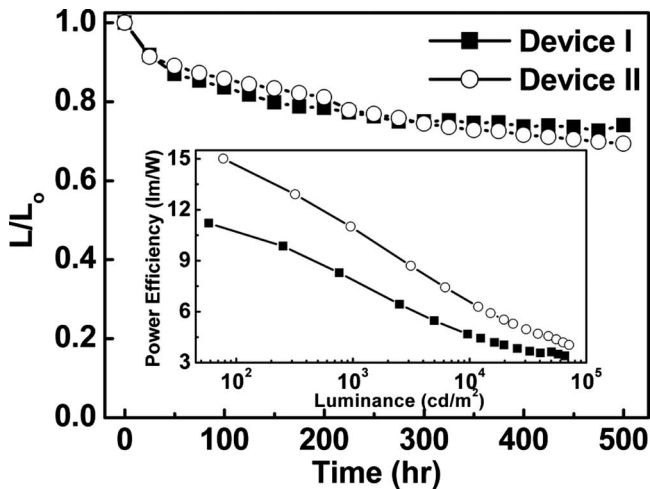


FIG. 5. Operational stability of devices I and II. Inset: power efficiency versus luminance characteristics of devices I and II.

plots the power efficiency against luminance for devices I and II. The power efficiency of device II at 1000 cd/m<sup>2</sup> can be as high as 14.6 lm/W (at 3.3 V), suggesting that the injection of electrons from the cathode of this PAK2-doped ETL is efficient even at a low drive voltage. The operational lifetimes of devices I and II under a constant current density of 20 mA/cm<sup>2</sup> were also measured in a dry box, as shown in Fig. 5. The  $t_{70}$  (time for the luminance to decline to 70% of the initial luminance) values of both devices are approximately 500 h. Based on the assumption of scalable Coulombic degradation,<sup>18</sup> the half-lives ( $t_{1/2}$ ) of devices I and II can be projected to 28 900 and 36 200 h at 1000 cd/m<sup>2</sup>, respectively. The operational stability of device II with  $n$ -doped ETL is clearly comparable to that of conventional device I.

In summary,  $I$ - $V$  measurement and temperature-dependent AS indicated that the incorporation of PAK2 into BPhen increases the Fermi-level to only around 0.5 eV below BPhen's LUMO band, further enhancing the efficiency of electron injection from Al cathode. Additionally, the low deposition temperature of PAK2 substantially facilitates the fabrication processes. When this  $n$ -doped layer is incorporated in the OLED device, the C545T-doped device achieves a current efficiency of 16 cd/A and a power efficiency of 10.9 lm/W at 1000 cd/m<sup>2</sup>.

This work was supported by the National Science Council of Taiwan (NSC 96-2218-E-009-009) and Chunghwa Picture Tubes, Ltd. (CPT) of Taoyuan, Taiwan.

- <sup>1</sup>C. W. Tang and S. A. Vanslyke, *Appl. Phys. Lett.* **51**, 913 (1987).
- <sup>2</sup>L. S. Hung and M. G. Mason, *Appl. Phys. Lett.* **78**, 3732 (2001).
- <sup>3</sup>L. S. Hung, C. W. Tang, and M. G. Mason, *Appl. Phys. Lett.* **70**, 152 (1997).
- <sup>4</sup>P. He, S. D. Wang, S. T. Lee, and L. S. Hung, *Appl. Phys. Lett.* **82**, 3218 (2003).
- <sup>5</sup>C. Ganzorig and M. Fujihira, *Jpn. J. Appl. Phys., Part 2* **38**, L1348 (1999).
- <sup>6</sup>S. H. Kim, J. Jang, and J. Y. Lee, *Appl. Phys. Lett.* **91**, 103501 (2007).
- <sup>7</sup>J. Huang, M. Pfeiffer, A. Werner, J. Blochwitz, S. Liu, and K. Leo, *Appl. Phys. Lett.* **80**, 139 (2002).
- <sup>8</sup>G. F. He, O. Schneider, D. S. Qin, X. Zhou, M. Pfeiffer, and K. Leo, *J. Appl. Phys.* **95**, 5773 (2004).
- <sup>9</sup>J. H. Lee, M. H. Wu, C. C. Chao, H. L. Chen, and M. K. Leung, *Chem. Phys. Lett.* **416**, 234 (2005).
- <sup>10</sup>J. Kido and T. Matsumoto, *Appl. Phys. Lett.* **73**, 2866 (1998).
- <sup>11</sup>T. Hasegawa, S. Miura, T. Moriyama, T. Kimura, I. Takaya, Y. Osato, and H. Mizutani, Proceedings of the Society for Information Display, Seattle, Washington, 2004 (unpublished), p. 28.
- <sup>12</sup>M. T. Hsieh, C. C. Chang, J. F. Chen, and C. H. Chen, *Appl. Phys. Lett.* **89**, 103510 (2006).
- <sup>13</sup>W. G. Oldham and S. S. Naik, *Solid-State Electron.* **15**, 1085 (1972).
- <sup>14</sup>S. W. Tsang, S. K. So, and J. B. Wu, *J. Appl. Phys.* **99**, 013706 (2006).
- <sup>15</sup>S. Odermatt, N. Ketter, and B. Witzigmann, *Appl. Phys. Lett.* **90**, 221107 (2007).
- <sup>16</sup>M. Pfeiffer, K. Leo, and N. Karl, *J. Appl. Phys.* **80**, 6880 (1996).
- <sup>17</sup>H. Aziz, Z. D. Popovic, N.-X. Hu, A.-M. Hor, and G. Xu, *Science* **283**, 1900 (1999).
- <sup>18</sup>S. A. Van Slyke, C. H. Chen, and C. W. Tang, *Appl. Phys. Lett.* **69**, 2160 (1996).